



**HAL**  
open science

## Topical treatment with a mu opioid receptor agonist alleviates corneal allodynia and corneal nerve sensitization in mice

Fanny Joubert, Adrian Guerrero-Moreno, Darine Fakih, Elodie Reboussin, Claire Gaveriaux-Ruff, Maria Carmen Acosta, Juana Gallar, José Alain Sahel, Laurence Bodineau, Christophe Baudouin, et al.

### ► To cite this version:

Fanny Joubert, Adrian Guerrero-Moreno, Darine Fakih, Elodie Reboussin, Claire Gaveriaux-Ruff, et al.. Topical treatment with a mu opioid receptor agonist alleviates corneal allodynia and corneal nerve sensitization in mice. *Biomedicine and Pharmacotherapy*, 2020, 132, pp.110794. 10.1016/j.biopha.2020.110794 . hal-03045488

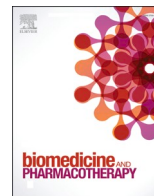
**HAL Id: hal-03045488**

**<https://hal.sorbonne-universite.fr/hal-03045488>**

Submitted on 8 Dec 2020

**HAL** is a multi-disciplinary open access archive for the deposit and dissemination of scientific research documents, whether they are published or not. The documents may come from teaching and research institutions in France or abroad, or from public or private research centers.

L'archive ouverte pluridisciplinaire **HAL**, est destinée au dépôt et à la diffusion de documents scientifiques de niveau recherche, publiés ou non, émanant des établissements d'enseignement et de recherche français ou étrangers, des laboratoires publics ou privés.



## Original article

# Topical treatment with a mu opioid receptor agonist alleviates corneal allodynia and corneal nerve sensitization in mice

Fanny Joubert<sup>a</sup>, Adrian Guerrero-Moreno<sup>a</sup>, Darine Fakih<sup>a,b</sup>, Elodie Reboussin<sup>a</sup>,  
 Claire Gaveriaux-Ruff<sup>c</sup>, Maria Carmen Acosta<sup>d</sup>, Juana Gallar<sup>d,e</sup>, José Alain Sahel<sup>a,f,g,h</sup>,  
 Laurence Bodineau<sup>i</sup>, Christophe Baudouin<sup>a,f,j</sup>, William Rostène<sup>a</sup>,  
 Stéphane Mélik-Parsadaniantz<sup>a</sup>, Annabelle Réaux-Le Goazigo<sup>a,\*</sup>

<sup>a</sup> Sorbonne Université, INSERM, CNRS, Institut de la Vision, 17 Rue Moreau, F-75012, Paris, France

<sup>b</sup> R&D Department, Laboratoires Théa, 12 Rue Louis Biérot, F-63000, Clermont-Ferrand, France

<sup>c</sup> Institut de Génétique et de Biologie Moléculaire et Cellulaire, Université de Strasbourg, CNRS, UMR7104, INSERM U1258, Ecole Supérieure de Biotechnologie de Strasbourg, Illkirch, Strasbourg, France

<sup>d</sup> Instituto de Neurociencias Universidad Miguel Hernández-CSIC, San Juan de Alicante, Alicante, Spain

<sup>e</sup> Instituto de Investigación Sanitaria y Biomédica de Alicante, Alicante, Spain

<sup>f</sup> CHNO des Quinze-Vingts, INSERM-DGOS CIC 1423, 28 Rue de Charenton, F-75012, Paris, France

<sup>g</sup> Fondation Ophthalmologique Rothschild, 29 Rue Manin, F-75019, Paris, France

<sup>h</sup> Department of Ophthalmology, The University of Pittsburgh School of Medicine, Pittsburgh, PA, 15213, United States

<sup>i</sup> Sorbonne Université, INSERM, UMR\_S1158 Neurophysiologie Respiratoire Expérimentale et Clinique, F-75013, Paris, France

<sup>j</sup> Department of Ophthalmology, Ambroise Paré Hospital, AP-HP, Paris-Saclay University, F-92100 Boulogne-Billancourt, France



## ARTICLE INFO

## Keywords:

Corneal pain  
 Inflammation  
 Opioid receptor  
 Electrophysiology

## ABSTRACT

Corneal pain is considered to be a core symptom of ocular surface disruption and inflammation. The management of this debilitating condition is still a therapeutic challenge. Recent evidence supports a role of the opioid system in the management of corneal nociception. However, the functional involvement of the mu opioid receptor (MOR) underlying this analgesic effect is not known. We first investigated the expression of the MOR in corneal nerve fibers and trigeminal ganglion (TG) neurons in control mice and a mouse model of corneal inflammatory pain. We then evaluated the anti-nociceptive and electrophysiological effects of DAMGO ([D-Ala<sup>2</sup>,N-Me-Phe<sup>4</sup>, Gly<sup>5</sup>-ol] enkephalin), a MOR-selective ligand. MOR immunoreactivity was detected in corneal nerve fibers and primary afferent neurons of the ophthalmic branch of the TG of naive mice. MOR expression was significantly higher in both structures under conditions of inflammatory corneal pain. Topical ocular administration of DAMGO strongly reduced both the mechanical (von Frey) and chemical (capsaicin) corneal hypersensitivity associated with inflammatory ocular pain. Repeated instillations of DAMGO also markedly reversed the elevated spontaneous activity of the ciliary nerve and responsiveness of corneal polymodal nociceptors that were observed in mice with corneal pain. Finally, these DAMGO-induced behavioral and electrophysiological responses were totally blunted by the topical application of naloxone methiodide, an opioid receptor antagonist. Overall, these results provide evidence that topical pharmacological MOR activation may constitute a therapeutic target for the treatment of corneal pain and improve corneal nerve function to alleviate chronic pain.

## 1. Introduction

Ocular pain, in particular, cornea-driven pain, is considered to be a core symptom of inflammatory and traumatic disorders of the ocular surface. Pain is a frequently reported symptom in dry eye disease, which has gained recognition as a public health problem, given its increasing

prevalence (5–30% of the population aged  $\geq 50$  years), morbidity, and associated social burden [1–4]. The management of chronic corneal pain still represents a therapeutic challenge. The cornea is one of the most densely innervated and sensitive tissues in the body [5,6]. Its sensory innervation is supplied by ciliary nerves derived from ophthalmic division of the trigeminal ganglion (TG) [7–9]. The cornea is exclusively

\* Corresponding author.

E-mail address: [annabelle.reaux@inserm.fr](mailto:annabelle.reaux@inserm.fr) (A. Réaux-Le Goazigo).

<https://doi.org/10.1016/j.bioph.2020.110794>

Received 6 August 2020; Received in revised form 17 September 2020; Accepted 19 September 2020

Available online 6 October 2020

0753-3322/© 2020 The Author(s).

Published by Elsevier Masson SAS. This is an open access article under the CC BY-NC-ND license

(<http://creativecommons.org/licenses/by-nc-nd/4.0/>).

innervated by C- and A-delta fibers, including mechano-nociceptors, which are triggered by noxious mechanical stimulation, polymodal nociceptors, which are excited by mechanical, chemical, and thermal stimuli, and cold thermoreceptors, which are activated by cooling [10–12].

Inflammatory pain refers to increased sensitivity due to the inflammatory response associated with tissue damage. Corneal inflammation is a reaction of the immune system to pathogens or injuries, whereas the triggers of ocular inflammation in the clinic may be different (dry eye disease, breakdown of corneal epithelium, uveitis, etc.). However, they produce similar symptoms, including pain. Pain can be modulated by endogenous (enkephalins, endorphins, and dynorphins) and exogenous (opium alkaloids) opioids, which activate mu-(MOR), delta-(DOR) and kappa-(KOR) opioid receptors expressed throughout the peripheral and central nervous systems [13–16]. Although systemic opioids are still the gold standard for treating pain, common side effects include respiratory depression, nausea, constipation, hyperalgesia, addiction, tolerance, and dependence [17]. In ophthalmology, oral opioids are used for post-operative pain [18] and for alleviating corneal neuropathic pain in dry-eye patients [19,20], but side effects are often reported. Topical ocular drug administration offers a number of advantages over systemic administration, including direct targeting of the corneal nerves by the drugs and minimizing centrally mediated side-effects. We recently reported that repeated instillation of PL265, a dual enkephalinase inhibitor, which increases the endogenous levels of enkephalins, mediates antinociceptive effects in corneal pain models [21]. Moreover, studies have considered topical morphine as a safe alternative to alleviate corneal nociception in rats [22], cats [23], dogs [24], and patients [25, 26]. However, these studies did not evaluate the functional implication of the MOR underlying this analgesic effect, nor its expression in corneal nerves and trigeminal neurons or the electrophysiological effects of a topical MOR agonist on corneal nerve activity.

Given that selective MOR agonists can be particularly effective for the treatment of inflammatory pain [27], we hypothesized that targeting corneal MOR by topical agonists could be an efficient means to alleviate corneal inflammatory pain in mice and modulate corneal nerve-fiber activity.

Herein, we report increased expression of the MOR in corneal nerve fibers and trigeminal sensory neurons in a mouse model of inflammatory corneal pain. We further demonstrate numerous beneficial effects of multiple instillations of DAMGO ([D-Ala<sup>2</sup>,N-Me-Phe<sup>4</sup>,Gly<sup>5</sup>-ol] enkephalin), a MOR-selective ligand, on mechanical and chemical corneal allodynia, as well as on spontaneous and evoked-ciliary nerve-fiber activity. Finally, through the use of the pharmacological antagonist, naloxone methiodide, we confirmed that these effects are specifically mediated by peripheral MORs. Our experiments have important implications for the potential role of MOR agonists as anti-allodynic drugs and for understanding how mu opioid agonists modulate corneal nerve-fiber activity in the context of corneal pain.

## 2. Materials and methods

### 2.1. Animals

Six-week-old adult male C57BL/6 mice (Janvier Labs, Le Genest Saint Isle, France) were randomly assigned to cages (5 mice/cage) and maintained on a 12 h light–dark cycle with free access to food and water. All experiments were approved by the Charles Darwin Ethics Committee for Animal Experimentation (Ce5/2011/05) and carried out in accordance with Directive 2010/63/EU of the European Parliament and the Council of 22 September 2010 and French law (2013/118). They were also validated by the “Service Protection et Santé Animales”, APAFIS #1501 2015081815454885 v2. All efforts were made to minimize the number of animals used and their suffering. All experiments were performed in strict accordance with the recommendations of the Weatherall Report regarding good animal practice.

### 2.2. Drugs: pharmacological agents

DAMGO ([D-Ala<sup>2</sup>,N-Me-Phe<sup>4</sup>,Gly<sup>5</sup>-ol] enkephalin), naloxone methiodide, capsaicin, and lipopolysaccharide (LPS; from *Escherichia coli* O111:B4) were obtained from Sigma-Aldrich (Saint-Quentin Fallavier, France). DAMGO, naloxone methiodide and LPS were dissolved in 0.1 M phosphate-buffered saline (PBS; pH 7.4). Capsaicin (Sigma-Aldrich) was dissolved in 100 % ethanol (1 M solution) and then diluted in isotonic saline to obtain a 10 μM solution.

### 2.3. Preclinical mouse model of corneal inflammatory pain (corneal scraping + LPS administration)

Mice were anesthetized by isoflurane inhalation (2%). A drop of ophthalmic gel was used to maintain hydration of the left eye during the surgery. On day 1 (D1), the topical anesthetic oxybuprocaine (Théa laboratories, Clermont Ferrand, France) was applied to the ocular surface and corneal scraping was performed on the right eye using an interdental brush to remove the superficial corneal epithelium. Ten microliters LPS (5 mg/mL) was applied to the right scraped cornea immediately after corneal injury (D1), and a second LPS application was performed on D3, as previously described [21] (Supplementary Fig. 1A).

### 2.4. Topical ocular administrations: pharmacological studies

The effect of topical DAMGO (50 μM), a selective MOR ligand, was determined in a corneal inflammatory pain model. For topical ocular administration, the cage order was randomized daily. Animals received repeated instillation of PBS or naloxone methiodide (100 μM), followed by either PBS or DAMGO (50 μM) 10 min after, twice daily, for five consecutive days. Behavioral experiments and electrophysiological recordings were performed on D5, before (t<sub>0</sub>) and 15 min (t<sub>15</sub>) after the last drug instillation (Supplementary Fig. 1B).

### 2.5. In vivo confocal microscopy

Corneal integrity was examined by *in vivo* confocal microscopy (IVCM, Heidelberg Retina Tomography (HRT) II/Rostock Cornea Module [RCM; Heidelberg Engineering GmbH, Heidelberg, Germany]) as previously described [10,28]. The first layer of the superficial epithelium, the sub-basal plexus, and the stroma were observed. A minimum of 50 serial TIFF images (400 × 400 μm) were acquired per animal.

### 2.6. Electrophysiological experiments: Recording of spontaneous and stimulus-evoked ciliary nerve-fiber activity

Electrophysiological experiments were performed on the control and injured corneas on D5. The mice were sacrificed by cervical dislocation. Their eyes were enucleated and the connective tissue and extraocular muscles at the back of the eye carefully removed to expose and isolate the ciliary nerves. The eye was then placed in a two-compartment chamber (divided by a Sylgard-coated plastic wall) to isolate the cornea from the back of the eye, as previously described [10,29,30]. The cornea was continuously superfused with a deoxygenated physiological saline solution (133.4 mM NaCl, 4.7 mM KCl, 2 mM CaCl<sub>2</sub>, 1.2 mM MgCl<sub>2</sub>, 16.3 mM NaHCO<sub>3</sub>, 1.3 mM NaH<sub>2</sub>PO<sub>4</sub>, 7.8 mM glucose) at a rate of 2 mL/min at 33 ± 1 °C. It was then saturated with O<sub>2</sub> and adjusted to pH 7.4 by bubbling with 95 % O<sub>2</sub> and 5% CO<sub>2</sub>. The posterior compartment of the chamber was filled with physiological saline. The extracellular multi-unit electrical activity of the ciliary nerve was recorded using a suction electrode (Ag/AgCl). The signal was filtered (300–5000 Hz), amplified (x 10000) (A–M Systems, Sequim, USA), and digitalized using Spike 2 data analysis and acquisition software (CED Micro1401, Cambridge Electronic Design) at a sampling frequency of 10,000 Hz. A threshold corresponding to a +50 % peak to peak of the background noise was determined to distinguish the spike from noise, as previously

described [10]. The cornea was superfused with physiological saline for 30 min to stabilize the preparation before performing the electrophysiological recordings. The area of the corneal surface innervated by the recorded ciliary nerve (receptive field) was identified using mechanical stimulation with a fine paint brush, as previously described [10]. The following firing parameters were calculated: a) *Spontaneous activity*: after the stabilization period, the frequency of spontaneous activity was assessed as impulses per second (imp/s) for 1 min before any corneal stimulation; b) *Responsiveness to chemical (CO<sub>2</sub>) stimulation*: the following parameters were analyzed to describe the CO<sub>2</sub> pulse-evoked firing discharge: i) the mean firing frequency, expressed as the number of impulses per second (imp/s) for a 30-s CO<sub>2</sub> pulse and ii) the latency of the impulse discharge, in seconds, between the beginning of the CO<sub>2</sub> pulse and the first detected CO<sub>2</sub>-evoked nerve impulse.

Drugs were added to the physiological saline solution followed by incubation for 2 min, *i.e.*, either 1x PBS or DAMGO (50 μM) alone or naloxone methiodide (100 μM) followed by DAMGO (50 μM). The spontaneous and CO<sub>2</sub>-evoked activity were recorded and the perfusion then returned to a normal physiological saline solution. The spontaneous activity and corneal responsiveness to chemical stimulation at  $t_0$  and  $t_{15}$  after the last drug administration were compared (Supplementary Fig. 1B). Electrophysiological traces were analyzed in a blinded manner, the experimenter was blinded to the treatment (PBS, DAMGO, DAMGO + Naloxone Metiodide), as well as the group of mice analyzed (operated or naive).

## 2.7. Behavioral studies

Experiments were carried out during the light period (between 10:00 and 17:00). For behavioral tests, mice were placed in the testing room (at least 30 min before the start of the experiments) and the order of testing was randomized. The experimenter was blinded to the treatment group. Mice were trained a week before the surgery (surgery considered as D1 in this study). The immobilization (handling- restraint) lasted a maximum of 20 s to reduce any potential stress and anxiety.

*Corneal mechanical sensitivity*: von Frey filaments (Bioseb, Vitrolles, France) were used to evaluate corneal sensitivity in response to corneal mechanical stimulation [21,30]. The mechanical threshold response was determined by assessing the first blinking response evoked by calibrated von Frey filaments of increasing force (0.08–0.7 mN) applied to the central cornea of immobilized mice. The mechanical corneal sensitivity was determined on D1, before the surgery, to obtain the basal threshold. The  $t_0$  value determined on D5 corresponded to the mechanical threshold measured before the last daily PBS or DAMGO instillation. The  $t_{15}$  value corresponded to the threshold measured 15 min after the last topical administration of the drugs (Supplementary Fig. 1B).

*Corneal sensitivity to capsaicin*: The chemical corneal sensitivity to capsaicin was assessed by applying 10 μL of a 10 μM capsaicin solution to the cornea 15 min after the PBS or drug instillation, as previously described [21]. The animals were immediately placed in an individual cage and the palpebral closure time measured by the investigator. The same experimenter performed all experiments in a test room close to the colony room to minimize stress (Supplementary Fig. 1B).

## 2.8. Immunohistological studies

### 2.8.1. Tissue preparation

Mice were deeply anesthetized with a 300-μL mixture of ketamine (80 mg/kg) and xylazine (8 mg/kg), which was injected intraperitoneally. Mice were then perfused with a 0.9 % NaCl solution, followed by a 4% (mice) paraformaldehyde (PFA) solution. The eyes were enucleated and frozen in liquid nitrogen until use. The TG were carefully dissected, post-fixed for 24 h in 4% PFA and placed in a 30 % sucrose solution in PBS for 48 h before being frozen at –20 °C in 7.5 % gelatin and 10 % sucrose. Corneal and TG frozen sections were prepared using a Cryostat

(Leica Microsystems, Wetzlar, Germany). The sections were mounted on Superfrost™ slides and stored at –20 °C for subsequent use (Table 1).

### 2.8.2. Double immunofluorescence labelling in the cornea and TG

The suppliers, reference, and dilutions of the primary and secondary antibodies used for immunohistochemistry are listed in Table 1. Neuronal markers (PGP 9.5, anti-beta III tubulin and Milli-Mark Pan Neuronal Marker) were used to identify corneal nerves and trigeminal neurons. They are all suitable for detecting myelinated and nonmyelinated nerve fibers in peripheral tissues and are commonly used to identify all nerve fibers in the cornea [7,31–33]. We carefully checked that all of the neuronal markers showed classic morphological patterns and normal distribution of nerve fibers in the cornea tissues. Moreover, the beta III tubulin antibody stained cells exhibiting the classic morphology and distribution of neurons and their fibers in TG sections from mice.

The specificity of the MOR antibody: rabbit recombinant anti-Mu opioid receptor monoclonal antibody [UMB3, ab134054, abcam], has been previously well characterized [34]. This antibody was raised against a synthetic peptide corresponding to amino acids of human MOR aa 350–450 (the intracellular C-terminus). It is considered to be an excellent tool for assessing MOR protein expression in mice, rats, and human tissues and is widely used [15,35]. This antibody has also been knockout validated, as western-blot analysis of mouse brain homogenates from wild-type mice resulted in a broad band of ~70–80 kDa but not those from MOR knockout mice [34]. In addition, it provides specific staining of MOR-transfected cells and wild-type mouse brain and the translocation of MOR immunostaining after agonist exposure [34]. The absence of non-specific staining by the secondary antibody was demonstrated by incubating corneal and TG sections from naive and scraped/LPS-treated animals with a purified rabbit IgG Isotype control (Biorad, PRABP01) using the same concentration as that used with UMB3 for the corneal and TG sections. This was followed by incubation with the appropriate secondary antibodies and detection reagents (as described above). The sections were then analyzed in a blinded manner (Supplementary Fig. 2). Negative controls were included in which the primary antibodies were omitted to confirm secondary antibody specificity (data not shown).

*Corneal sections*: Sequential immunostaining was performed on whole-mount corneas and frozen corneal sections (12-μm cryostat sections). The corneas were rinsed in phosphate-buffered saline-0.1 % Triton (PBS-T 0.1 %) and blocked for 2 h at room temperature (RT) with PBS-T 0.1 % containing 10 % normal goat serum (NGS). The corneas were first incubated with monoclonal mouse anti-PGP 9.5 (ab8189, Abcam, Cambridge, UK, 1:500) (free-floating cornea) or an antibody against the pan neuronal marker (MAB2300, Millipore, 1:500) (cryostat sections) in PBS-T 0.5%–3% NGS overnight at 4 °C. The corneas were then rinsed in PBS-T 0.1 % and incubated with goat anti-mouse Alexa 488 (Invitrogen, 1:1000) and DAPI (1:1000) in PBS-T 0.5 %–3 % NGS for 2 h at RT. The corneas were washed in PBS-T 0.1 % and next incubated with rabbit monoclonal anti-MOR (UMB-3, ab134054, Abcam, Cambridge, UK, 1:250) in PBS-T 0.5 %–3 % NGS for 24 (cryostat sections) or 36 h (free-floating cornea) at 4 °C. The tissues were rinsed and incubated with donkey anti-rabbit Alexa 594 (Invitrogen, 1:1000) in PBS-T 0.5 %–3 % NGS for 2 h at RT. Free-floating corneas were mounted onto Superfrost™ slides and the slides cover slipped with Fluoromount Aqueous Mounting Medium (Sigma Aldrich).

*TG sections*: frozen TG sections were rinsed in PBS-T 0.1 % and blocked for 2 h with PBS-T 0.1 % containing 3% normal horse serum (NHS). The sections were incubated with a solution containing a mixture of primary antibodies (rabbit monoclonal anti-MOR, 1:500; mouse monoclonal anti-beta III tubulin antibody, ab78078, Abcam; 1:500) in PBS-T 0.5 % with 3% NHS for 48 h. The sections were rinsed in PBS-T 0.1 % and the slides incubated with biotinylated goat anti-rabbit immunoglobulin (Vector Laboratories, 1:1000) and donkey anti-mouse Alexa 488 antibody (Invitrogen, 1:500) in PBS-T 0.5 % for 2 h at RT. Then, TG

**Table 1**  
Suppliers, references, and dilutions of the primary and secondary antibodies used for immunohistochemistry.

Sample	Sectioning	Primary Antibody (target, ref#, company)	Concentration		Secondary Antibody	Ratio	Amplification
			Used	Real			
Cornea	No (whole-mount)	PGP 9.5, ab8189, Abcam	1:500	2 ug/mL	goat anti-mouse Alexa 488, Invitrogen	1:1000	
		MOR, UMB-3, ab134054, Abcam	1:250	0,176 ug/mL	donkey anti-rabbit Alexa 594, Invitrogen	1:1000	
	Cryostat (14 µm)	Pan Neuronal marker, MAB 2300, Millipore	1:500	Unknown	goat anti-mouse Alexa 488, Invitrogen	1:1000	
		MOR, UMB-3, ab134054, Abcam	1:250	0,176 ug/mL	donkey anti-rabbit Alexa 594, Invitrogen	1:1000	
TG	Cryostat (16 µm)	MOR, UMB-3, ab134054, Abcam	1:50	0,88 µg/mL	goat anti rabbit biotinylated, Vector Laboratories	1:1000	Streptavidin Alexa 594 conjugated, Invitrogen (1:1000)
		beta III Tubulin, ab78078, Abcam	1:500	2 ug/mL	donkey anti-mouse Alexa 488, Invitrogen	1:500	

sections were incubated with Alexa 594-conjugated streptavidin (Invitrogen, 1:1000) and DAPI (1:1000) in PBS-T 0.5 % for 2 h at RT. The sections were washed, mounted onto Superfrost™ slides, and cover slipped with Fluoromount.

### 2.9. Fluorescent in situ hybridization for Mu opioid receptor mRNA in mouse TGs

Mouse TGs were dissected and post-fixed in 4% PFA for 24 h at 4 °C. The tissues were immersed in 10 %, 20 %, and 30 % sucrose solutions (in PBS) for 12–24 h at each step. The tissues were placed at an optimal cutting temperature (OCT), frozen in liquid nitrogen, and stored at -80 °C. Then, the TG were cut using a cryostat (Leica CM 3050 S) to make 12-µm sections, which were mounted on Superfrost slides. Fluorescent *in situ* hybridization studies were performed using the RNAscope Fluorescent Multiplex Reagent kit v2 assay, according to the protocol for fixed frozen tissue (Advanced Cell Diagnostics, Newark, CA). Briefly, the sections were washed with 1X PBS, treated with hydrogen peroxide (RNAscope, ref# 322335) for 10 min at RT and then washed in distilled H<sub>2</sub>O. Using a steamer, the tissues were treated with distilled H<sub>2</sub>O for 10 s at 99 °C and then moved to RNAscope 1X target Retrieval Reagent (RNAscope, ref# 322000) and incubated for 5 min at 99 °C. The tissues were washed with distilled H<sub>2</sub>O, transferred to 100 % ethanol for 3 min and treated with RNAscope Protease III (RNAscope, ref#322337) for 30 min at 40 °C. A species-specific target probe for MOR, Oprm1-C3 (ref# 315841-C3), was diluted (1:50) with probe diluent (RNAscope, ref#300041). The sections were then incubated with the Oprm1-C3 probe and negative (ref# 320871) and positive (ref# 320881) control probes (provided by the manufacturer). The probes were hybridized for 2 h at 40 °C in a humidified oven (RNAscope HybEZ oven, with an HybEZ humidity control tray from Advanced Cell Diagnostics). A series of incubations was then performed to amplify the hybridized probe signal and label the target probe for the assigned fluorescence detection channel (PerkinElmer, Opal 650 Reagent, Ref# FP1496A; dilution 1:200). The nuclei were stained using a DAPI nuclear stain (RNAscope Ref# 323108) for 30 s at RT. The slides were then mounted using Prolong Gold Antifade Mounting reagent (Ref# P36934) onto glass slides and cover slipped.

Expression of the MOR gene and protein was quantified by examining the corneal and TG sections with a Zeiss M1 epifluorescence microscope (Axio ImagerM1; Carl Zeiss) equipped with a digital camera (Axio Cam HRC; Carl Zeiss) and image acquisition software (Zen; Carl Zeiss). The microscope settings were established using a control section and remained unchanged for all subsequent acquisitions. TIFF images were recorded. Three to five sections were used for the cornea and TG for each animal. Images (grayscale 8-bits) were then analyzed using Fiji (ImageJ) software. The thresholding function was used to discriminate objects of interest from the surrounding background and the total surface occupied by immunoreactive structures (*i.e.*, the total stained

pixels) above the set threshold was estimated within a standard area, as previously reported [21]. A summation of all grey values for the entire image was extracted for the TG sections.

### 2.10. Microscopic analysis

Tissue sections were examined with an inverted Olympus FV1000 confocal microscope equipped with an argon (488 nm) ion laser and laser diodes (405 and 559 nm). The images were acquired sequentially, line-by-line, to reduce excitation and emission crosstalk. The step size was defined according to the Nyquist–Shannon sampling theorem (1024\*1024 pixels). A PlanApoN (20/1.42 NA, oil immersion) objective lens (Olympus) was used and TIFF images were obtained. A single investigator analyzed all data from the microscopic analysis in a blinded manner.

### 2.11. Statistical analysis

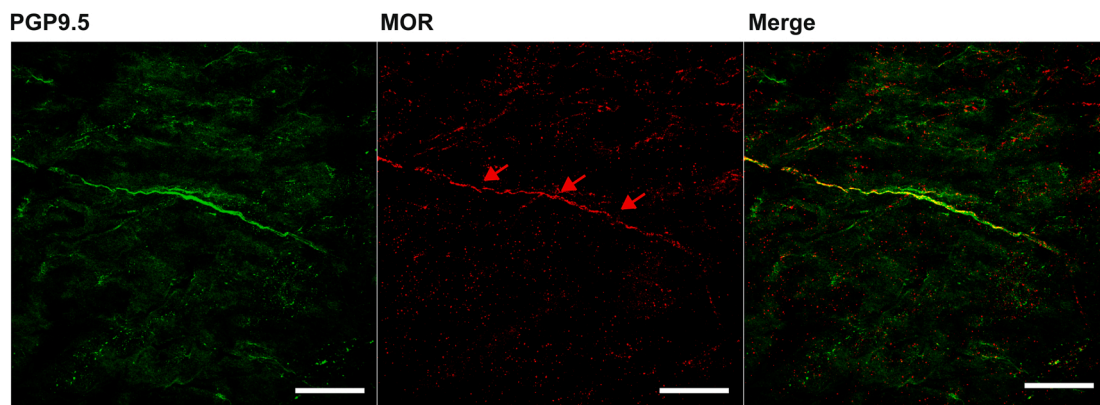
The data are expressed as the mean ± SEM and were analyzed using GraphPad Prism7 (GraphPad, San Diego California USA). The normality of the data distribution was verified using the Kolmogorov–Smirnov test. Paired or unpaired *t* tests or Mann–Whitney tests were used to assess differences for the inflammatory corneal injury model. For the DAMGO experiments, a Kruskal–Wallis test, followed by Dunn's post hoc least squares differences (PLSD) correction, or one-way or two way ANOVA, followed by Bonferroni's PLSD correction, was performed, depending on which was appropriate. The differences were considered significant for  $p < 0.05$ .

## 3. Results

### 3.1. MOR is expressed in the corneal nerve fibers and trigeminal primary sensory neurons in mice

We carried out immunohistochemistry experiments to determine whether MOR is expressed in the corneal nerve fibers and primary afferent neurons of the ophthalmic branch of the TG in control mice. MOR immunoreactivity was clearly detectable in PGP9.5-positive nerve fibers in mouse cornea (Fig. 1A). We also found MOR immunoreactivity in numerous primary sensory neuron somata (positive for beta III tubulin), located in the ophthalmic branch of the TG in mice (Fig. 1B). Moreover, MOR immunoreactivity was predominantly detected in primary sensory neurons of small (diameter < 25 µm) to medium (25–45 µm) size. The presence of the MOR in the corneal nerve fibers and afferent primary neurons of the ophthalmic branch of the TG under physiological conditions led us to further investigate the functional role of this receptor under conditions of inflammatory corneal pain.

A



B

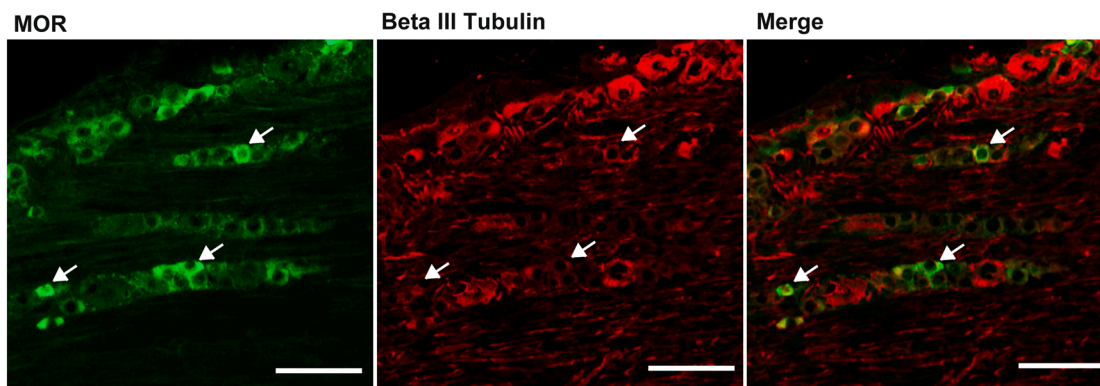


**Fig. 1.** Mu opioid receptor immunoreactivity in corneal nerves and primary afferent neurons in the TG of control mice.

(A) Confocal images showing MOR immunoreactivity in mouse corneal nerve fibers immuno-stained with the PGP9.5 neuronal marker (red arrows). Scale bar: 25  $\mu\text{m}$ . (B) Images showing immunofluorescent staining for the MOR and beta III tubulin in the ophthalmic branch of the TG. Arrows indicate afferent TG sensory neurons labelled by the MOR UMB3 antibody. Note the presence of MOR immunoreactivity in small- and medium-sized neurons. Scale bar: 100  $\mu\text{m}$ .

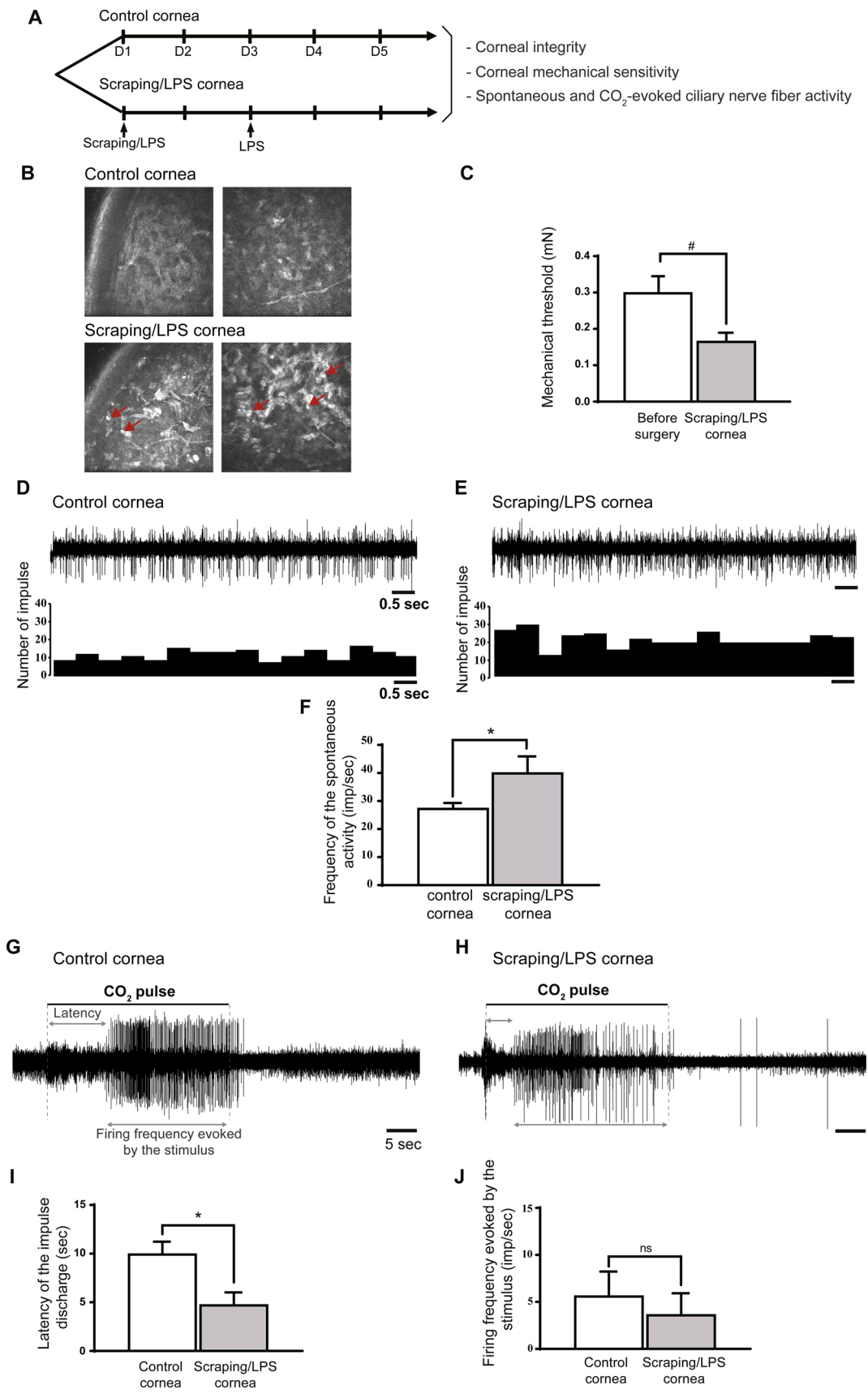
### 3.2. Scraping/LPS animals exhibit alterations of the corneal integrity, mechanical corneal sensitivity, and ciliary nerve fiber activity

We modelled corneal inflammatory pain using the scraping/LPS model that we previously developed and characterized [21]. Corneal scraping (*i.e.*, corneal nerve damage) was performed on day 1 (D1), combined with two instillations of LPS (50  $\mu\text{g}$ ) on D1 and D3, as previously described [21]. On D5, corneal integrity was evaluated in control and scraping/LPS mice by *in vivo* confocal microscopy (IVCM) (Fig. 2A). IVCM images taken on D5 for the corneal scraping/LPS mice clearly confirmed the presence of numerous hyper-reflective inflammatory cells in the corneal stroma (Fig. 2B, red arrows) and corneal inflammation in this model. We then evaluated mechanical corneal sensitivity using von Frey filaments for both groups of animals. On D1, before corneal scraping, the baseline mechanical threshold response was  $0.30 \pm 0.04$  mN and was significantly lower than the basal values for the scraping/LPS-treated mice on D5 ( $0.17 \pm 0.02$  mN vs  $0.30 \pm 0.04$  mN,  $p < 0.05$ , Fig. 2C), demonstrating the development of mechanical allodynia. We further evaluated whether inflammatory pain provoked changes of corneal nerve activity. Electrophysiological recordings of the ciliary nerve fibers showed differences between the control (Fig. 2D) and scraping/LPS (Fig. 2E) corneas. Indeed, quantification of the electrophysiological recordings showed significantly higher spontaneous ciliary nerve activity on D5 for scraping/LPS mice than control animals ( $40.1 \pm 5.8$  imp/s vs  $27.4 \pm 1.9$  imp/s,  $p < 0.05$ ; Fig. 2D, E, and F). Next,

we investigated the responsiveness of polymodal corneal nociceptors using 30-s  $\text{CO}_2$  pulses applied to control and scraping/LPS corneas. The latency of the impulse discharge evoked by the  $\text{CO}_2$ -pulse was significantly shorter for the scraping/LPS ( $4.7 \pm 1.3$  s) than control corneas ( $10.0 \pm 1.2$  s,  $p < 0.05$ ; Fig. 2G, H, and I), indicating greater corneal responsiveness following corneal injury. There was no statistical difference in the firing frequency evoked by the stimulus between groups ( $5.6 \pm 1.0$  imp/s in control corneas vs  $3.6 \pm 0.9$  imp/s in scraping/LPS corneas, Fig. 2J).

### 3.3. Inflammatory corneal pain induces the upregulation of MOR expression in the cornea and trigeminal ganglion

Previous studies focusing on the spinal cord and dorsal root ganglia reported an increase in the peripheral expression of the MOR following inflammatory pain [36]. We investigated whether such modulation of the MOR also occurs in the corneal nerve fibers and trigeminal neurons of mice with corneal inflammatory pain (Fig. 3A). DAPI staining clearly confirmed alteration of the cornea, with cell infiltration in the stroma (red arrows) of the scraping/LPS mice relative to control corneas (Fig. 3B). This result corroborates *in vivo* confocal microscopy images of the cornea (see Fig. 3B) and is consistent with our previous results [21]. MOR immunoreactivity was higher in scraping/LPS than control corneas (Fig. 3B and C). Semi-quantitative analysis of MOR staining showed the stained area to be significantly greater in scraping/LPS than control



(caption on next page)

**Fig. 2.** Corneal inflammatory pain induces mechanical allodynia and increases the spontaneous and evoked activity of ciliary nerve fibers. (A) Schematic diagram of the experiments. (B) *In vivo* confocal images (400  $\mu\text{m}/400 \mu\text{m}$ ) of the control and scraping/LPS corneas on D5. Damage to the superficial epithelium and inflammatory cells (red arrows) was observed in the scraping/LPS corneas relative to the control (non-injured) corneas. (C) Histogram showing the corneal mechanical sensitivity threshold, measured using von Frey filaments, which elicited a different blink response before surgery (white bar) and 5 days (D5) after corneal scraping/LPS (grey bar). (D-E) Traces illustrating the multiunit spontaneous ciliary nerve activity in the control (D) and scraping/LPS (E) corneas. (F) Histogram showing the mean value of the multiunit spontaneous firing frequency of the ciliary nerve fibers in the control corneas (white bar) and on D5 after corneal scraping/LPS (grey bar). (G-H) Traces illustrating the corneal responsiveness to a 30-s  $\text{CO}_2$  pulse in control (G) and scraping/LPS (H) corneas. The black horizontal line represents the duration of the  $\text{CO}_2$  pulse. (I-J) Histograms showing the latency of the impulse discharge (I) and the mean firing frequency evoked by the  $\text{CO}_2$  stimulus (J) in the control corneas (white bars) and 5 days after corneal scraping/LPS (grey bars).  $N = 7-10$  mice per group. Differences were analyzed using paired *t* or Mann-Whitney tests, depending on which was appropriate. \* indicates a significant difference between the control and scraping/LPS groups. \*  $p < 0.05$ .

corneas ( $3.55 \pm 0.40\%$  vs  $1.35 \pm 0.06\%$ ,  $p < 0.001$ , Fig. 3D). We hypothesized that corneal inflammation may also increase gene expression of MOR mRNA in the ophthalmic part of the TG. We thus investigated the expression of MOR mRNA in the ipsilateral ophthalmic branch of the TG using RNAscope® *in situ* hybridization on control and scraping/LPS mice (Fig. 4A, B). Images of fluorescent *in situ* hybridization showed abundant red punctate dots, corresponding to RNAscope MOR probes, in numerous trigeminal primary sensory neurons (Fig. 4B). *In situ* hybridization also confirmed that MOR mRNA expression was found in small- and medium-sized sensory neurons. Moreover, we detected MOR mRNA expression in the cytoplasm of primary sensory neurons, suggesting that MOR mRNA is readily available to be translated into protein.

We next performed semi-quantitative analysis of MOR expression in the ophthalmic part of the TG to determine whether corneal pain affects trigeminal MOR expression. Semi-quantitative analysis of the area covered by the MOR mRNA probe, as well as staining intensity, showed MOR mRNA expression to be significantly higher in the TG from scraping/LPS mice than those of control animals (intensity:  $1.5 \times 10^6 \pm 0.2 \times 10^6$  AU vs  $0.9 \times 10^6 \pm 0.1 \times 10^6$  AU,  $p < 0.05$ ; area:  $7.6 \pm 0.8\%$  vs  $4.8 \pm 0.8\%$ ,  $p < 0.05$ ; Fig. 4C). Overall, these results show upregulation of the MOR in TG under conditions of corneal inflammatory pain.

### 3.4. Repeated topical treatment with DAMGO reduces spontaneous and stimulus-evoked ciliary nerve-fiber activity in the inflammatory corneal pain model

We further evaluated the chronic effects of *in vivo* instillation of DAMGO twice a day for five days on spontaneous (ongoing) ciliary nerve-fiber activity on the last day (D5) (Fig. 5A). On D5, before the last instillation of PBS or DAMGO alone (50  $\mu\text{M}$ ), or naloxone methiodide (100  $\mu\text{M}$ )/DAMGO (50  $\mu\text{M}$ ), the eyes were prepared for electrophysiological recordings. The basal spontaneous activity ( $t_0$  values) on D5 was significantly lower in the *in vivo* DAMGO-treated scraping/LPS than PBS-treated scraping/LPS corneas ( $32.0 \pm 4.5$  imp/s vs  $48.4 \pm 5.5$  imp/s,  $p < 0.05$ ) (Fig. 5B). The last DAMGO exposure did not modify the spontaneous ciliary nerve activity, which remained significantly lower than that of PBS-superfused corneas ( $t_{15}$  values:  $28.7 \pm 5.1$  imp/sec and  $54.9 \pm 7.2$  imp/sec,  $p < 0.01$ ; Fig. 5B, C, and D). Repeated topical naloxone methiodide administration prevented the inhibitory effects of DAMGO at  $t_0$  ( $51.2 \pm 2.7$  imp/s vs  $32.0 \pm 4.5$  imp/s,  $p < 0.01$ , Fig. 5B) and the effect was also observed 15 min after the last naloxone methiodide superfusion ( $45.6 \pm 2.3$  imp/s vs  $28.7 \pm 5.1$  imp/s,  $p < 0.05$ , Fig. 5B and E). These results confirm the involvement of opioid receptors at the ocular surface in the effects mediated by DAMGO.

The responsiveness of the polymodal corneal nerve fibers to chemical stimulation was thereafter evaluated on D5 at  $t_0$  and  $t_{15}$  after the last administration of either PBS, DAMGO (50  $\mu\text{M}$ ), or naloxone methiodide (100  $\mu\text{M}$ )/DAMGO (50  $\mu\text{M}$ ) (Fig. 6A, B, and C). At  $t_0$ , there was no significant difference in the latency between DAMGO- and PBS-treated animals ( $5.4 \pm 0.7$  s vs  $3.2 \pm 0.7$  s, Fig. 6B). In contrast, the latency was significantly higher 15 min after the last DAMGO application than for the PBS group ( $11.5 \pm 2.9$  s vs  $3.3 \pm 1.1$  s,  $p < 0.01$ ; Fig. 6B, D, and E). Furthermore, the  $t_{15}$  value for the DAMGO group was significantly higher than the  $t_0$  value ( $11.5 \pm 2.9$  s vs  $5.4 \pm 0.7$  s,  $p < 0.01$ ), confirming an additional effect of topical DAMGO on corneal nerve activity.

Finally, although there was no difference in the latency at  $t_0$  between the corneas treated with DAMGO and those treated with DAMGO and naloxone methiodide- ( $3.7 \pm 0.8$  s vs  $5.4 \pm 0.7$  s), naloxone methiodide exposure markedly blunted the increase of latency induced by DAMGO at  $t_{15}$  ( $3.9 \pm 1.1$  s vs  $11.5 \pm 2.9$  s,  $p < 0.001$ ; Fig. 6B, E, and F).

The firing frequency induced by a 30-s  $\text{CO}_2$  pulse before the last drug application ( $t_0$ ) was not significantly different between DAMGO- and PBS-treated corneas ( $2.4 \pm 0.6$  imp/s vs  $4.2 \pm 0.6$  imp/s, respectively, Fig. 6C). However, the last DAMGO application ( $t_{15}$ ) significantly reduced the firing frequency relative to that of PBS-treated corneas ( $1.9 \pm 0.4$  imp/s vs  $5.2 \pm 1.3$  imp/s relative to PBS superfusion,  $p < 0.05$ ; Fig. 6C, D, and E). The application of naloxone methiodide completely prevented the effects of DAMGO, both at  $t_0$  ( $5.7 \pm 1.1$  imp/s vs  $2.4 \pm 0.6$  imp/s,  $p < 0.05$ , Fig. 6C) and 15 min after the drug superfusion ( $5.9 \pm 1.2$  imp/s vs  $1.9 \pm 0.4$  imp/s,  $p < 0.05$ ; Fig. 6C, E, and F).

### 3.5. Repeated topical treatment with DAMGO reduces mechanical and chemical hypersensitivity of scraping/LPS mice

We then explored whether chronic administration of topical DAMGO could alleviate the corneal mechanical allodynia associated with scraping/LPS. The mechanical threshold response was measured using von Frey filaments, before surgery (basal values in naïve mice) and on D5 (at  $t_0$  and  $t_{15}$  after the last drug instillation) (Fig. 7A). Before surgery (naïve animals), there was no significant difference in the mechanical threshold between the animals ( $0.31 \pm 0.03$  mN,  $0.27 \pm 0.03$  mN, and  $0.26 \pm 0.03$  mN for the PBS, DAMGO, and naloxone methiodide/DAMGO groups, respectively) (Fig. 7B). Although the mechanical threshold was similar between DAMGO-treated mice and those of the PBS group at  $t_0$  on D5 ( $0.30 \pm 0.03$  mN vs  $0.22 \pm 0.02$  mN) (Fig. 7B), the mechanical threshold after the last DAMGO administration was significantly higher (less mechanical allodynia) 15 min. after its topical instillation than that of PBS ( $0.46 \pm 0.05$  mN vs  $0.24 \pm 0.02$  mN,  $p < 0.001$ ) (Fig. 7B). Further pharmacological experiments proved the involvement of corneal opioid receptors, as naloxone methiodide exposure completely blunted the effect of DAMGO at  $t_{15}$  ( $0.25 \pm 0.03$  mN vs  $0.46 \pm 0.05$  mN,  $p < 0.001$ ; Fig. 7B). Finally, we tested whether DAMGO is also able to reduce the nociceptive response induced by chemical stimulation by applying capsaicin (10  $\mu\text{M}$ ), the ligand of the transient receptor potential vanilloid 1 (TRPV1) channel, 15 min after the last instillation of PBS, DAMGO, or naloxone methiodide/DAMGO on D5. At D5, repeated topical DAMGO application resulted in significantly lower (by -25 %) palpebral closure time, an index of ocular discomfort/pain, than for animals receiving PBS ( $217.2 \pm 13.4$  s vs  $287.8 \pm 16.5$  s,  $p < 0.05$ , Fig. 7C). The topical instillation of naloxone methiodide completely prevented the antinociceptive effects of DAMGO ( $332.8 \pm 32.9$  s vs  $217.2 \pm 13.4$  s,  $p < 0.01$ , Fig. 7C), thus demonstrating that the analgesic effect of this  $\mu$  opioid agonist on capsaicin-evoked responses was mediated by opioid receptors expressed at the ocular surface. 4. DISCUSSION

Here, we show that (1) the MOR is detected in the corneal nerve fibers and trigeminal primary sensory neurons of mice, (2) inflammatory corneal pain induces upregulation of MOR expression in the cornea and TG, (3) topical administrations of DAMGO, a MOR-selective agonist, reduces mechanical allodynia and topical capsaicin-induced corneal



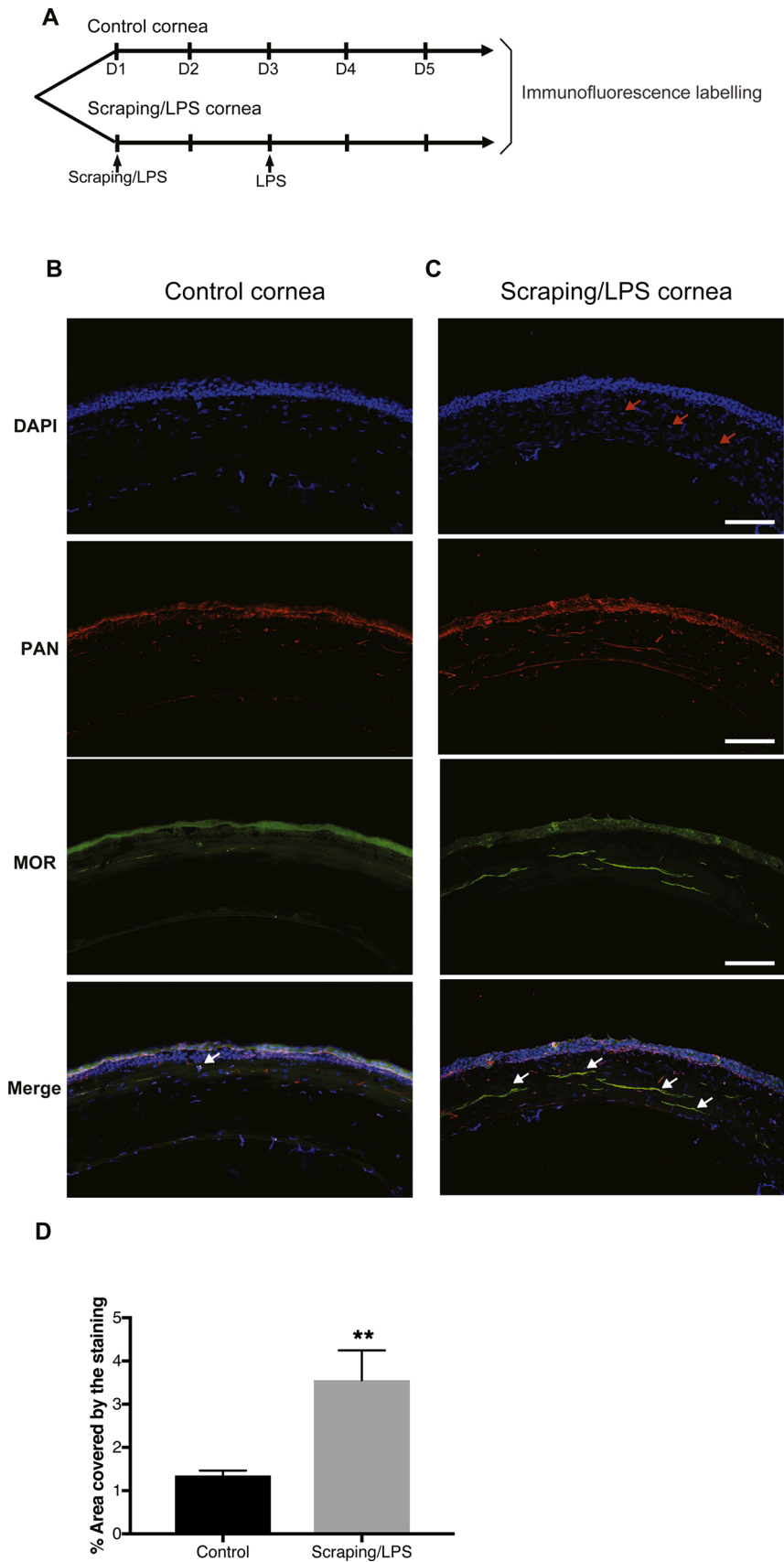


**Fig. 3.** MOR immunoreactivity increased in cornea under corneal pain conditions.

(A) Schematic diagram of the experiments. (B-C) Confocal images of control (B) and scraping/LPS (C) corneas stained with DAPI (blue), the PAN neuronal marker (red), and MOR antibodies (green). DAPI staining showed cell infiltration in the corneal stroma for the scraping/LPS mice (C, red arrows) relative to the control animals (B). Note that MOR immunoreactivity is higher in the inflamed (C, white arrows) than control cornea (B). Histograms showing the semi-quantitative analysis of the percentage of the area covered by MORs in control and scraping/LPS corneas (D). The difference between groups was analyzed using the unpaired *t* test. \*\* indicates a significant difference between the control and scraping/LPS groups. \*\**p* < 0.01. Scale bar: 100  $\mu$ m

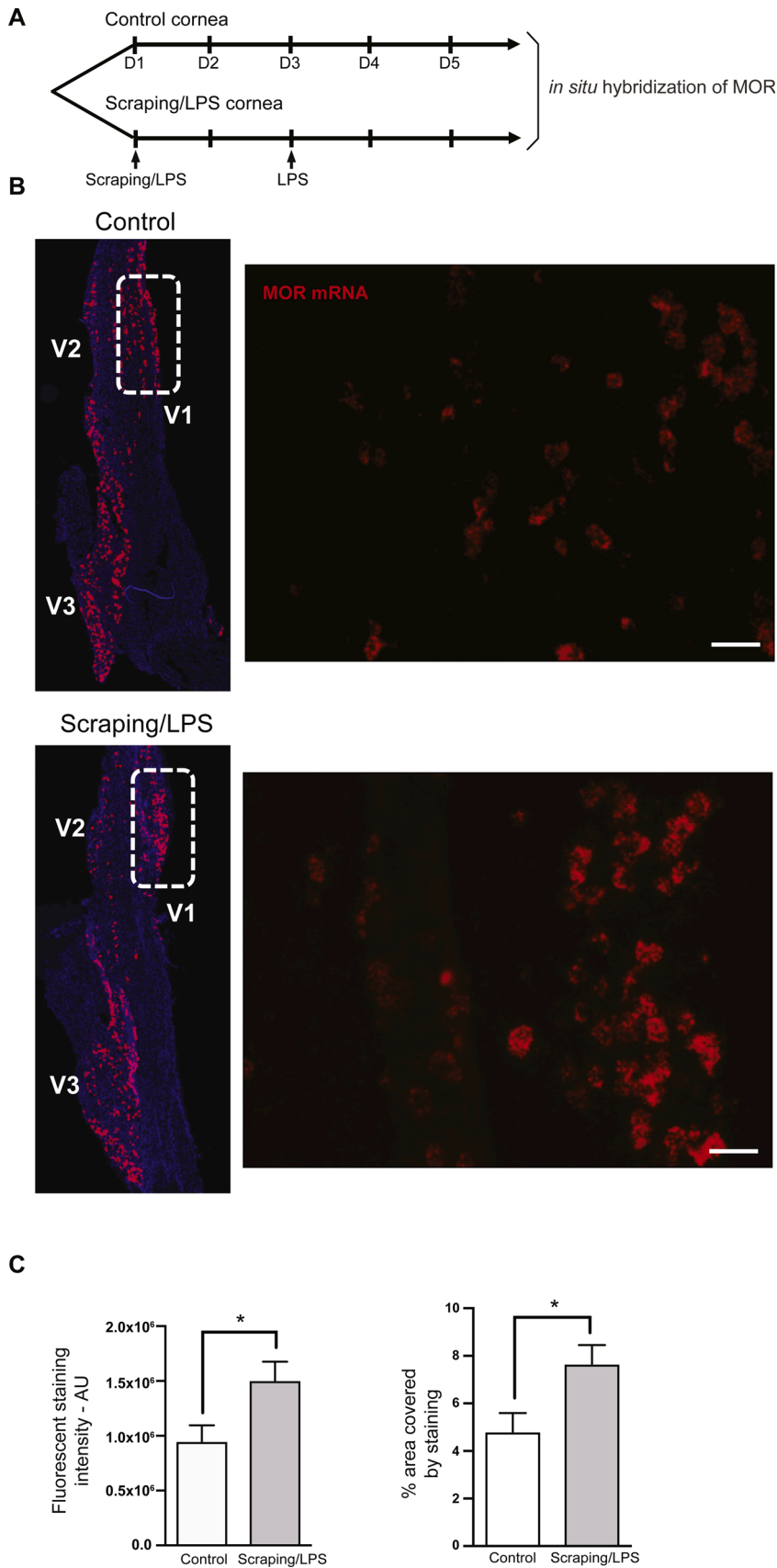


**Fig. 4.** Mu opioid receptor RNA expression increases in the trigeminal ganglion during inflammatory corneal pain. (A) Schematic diagram of the experiments. (B) MOR mRNA levels were evaluated by *in situ* hybridization RNAscope technology. Images for MOR mRNA (red) and nuclei counterstained with DAPI (blue) in the TG from control and scraping/LPS mice are shown. The dashed-line rectangle represents the ophthalmic branch (V1) of the TG. The high magnification shows the primary sensory neurons that express MOR mRNA in the ophthalmic branch of TG. Scale bars: 50  $\mu$ m. (C) Histograms showing the semi-quantitative analysis of the fluorescence staining intensity of MOR (left graph) and the percentage of area covered by MOR (right graph) in the ophthalmic branch of TG in control mice (white bars) and scraping/LPS animals (grey bars). MOR mRNA levels were analyzed using Fiji (ImageJ). N = 5 mice per group. The difference between groups was analyzed using an unpaired *t* test. \* indicates a significant difference between the control and scraping/LPS groups. \* *p* < 0.05. V1: ophthalmic branch, V2: maxillary branch, V3: mandibular branch of the TG.

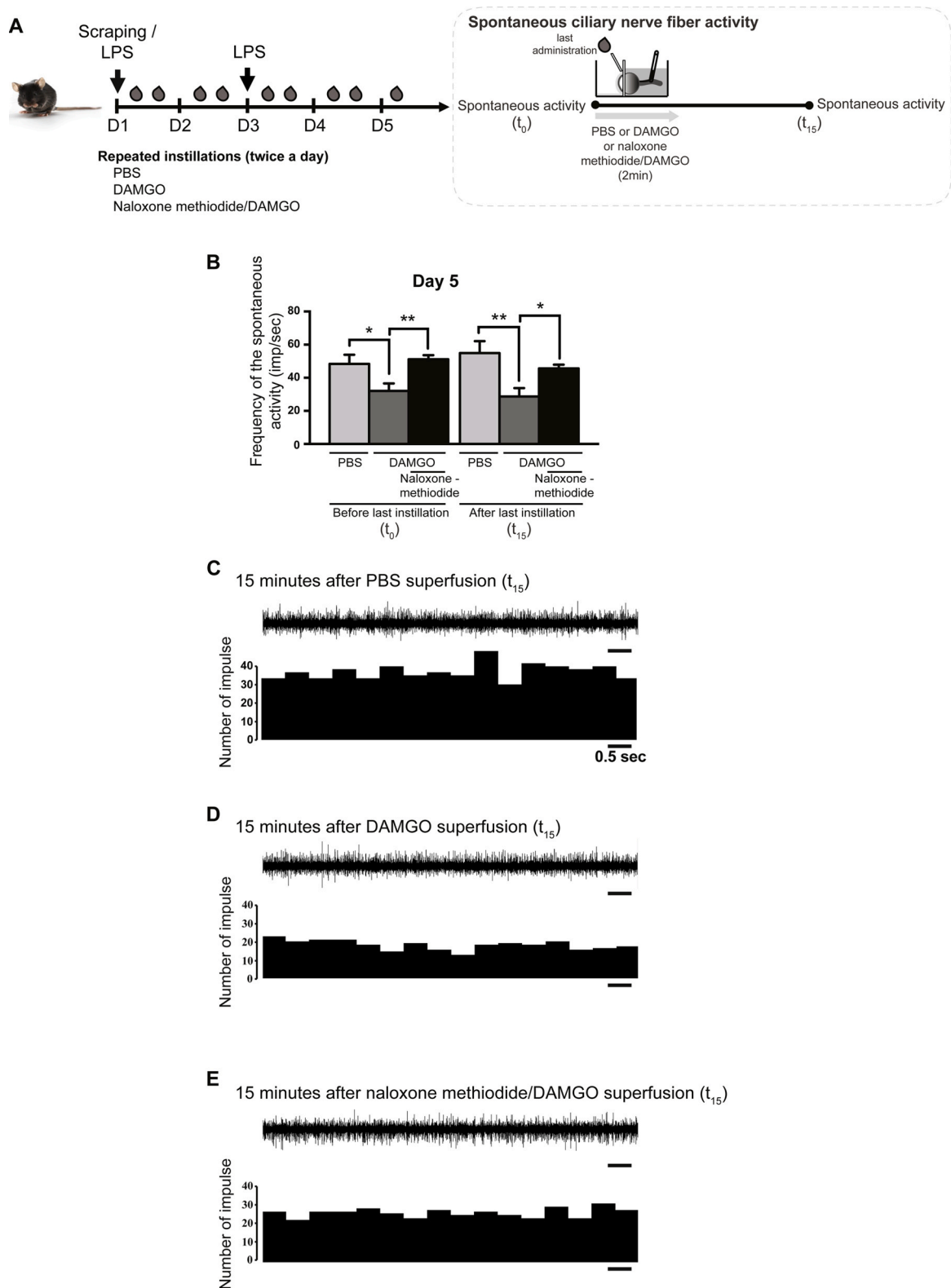


**Fig. 5.** Repeated topical instillations of DAMGO prevents the increase in spontaneous activity of ciliary nerve fibers induced by corneal pain. (A) Schematic diagram of the experiments. Spontaneous ciliary nerve-fiber activity was determined before ( $t_0$ ) and 15 min ( $t_{15}$ ) after the last drug exposure. (B) Histogram showing the mean value of the spontaneous firing frequency of ciliary nerve fibers on D5 at  $t_0$  and  $t_{15}$  after the last instillation of PBS (light grey bars), DAMGO (dark grey bars), or naloxone methiodide followed by DAMGO (black bars). (C–E) Traces illustrating the spontaneous ciliary nerve-fiber activity on D5 at  $t_{15}$  after the last instillation of PBS (C), DAMGO (D), or naloxone methiodide followed by DAMGO (E).  $N = 5-10$  mice per group. The differences between groups were analyzed by one-way ANOVA. \* indicates a significant difference between DAMGO and PBS alone or naloxone methiodide followed by DAMGO. \* $p < 0.05$ , \*\* $p < 0.01$ .

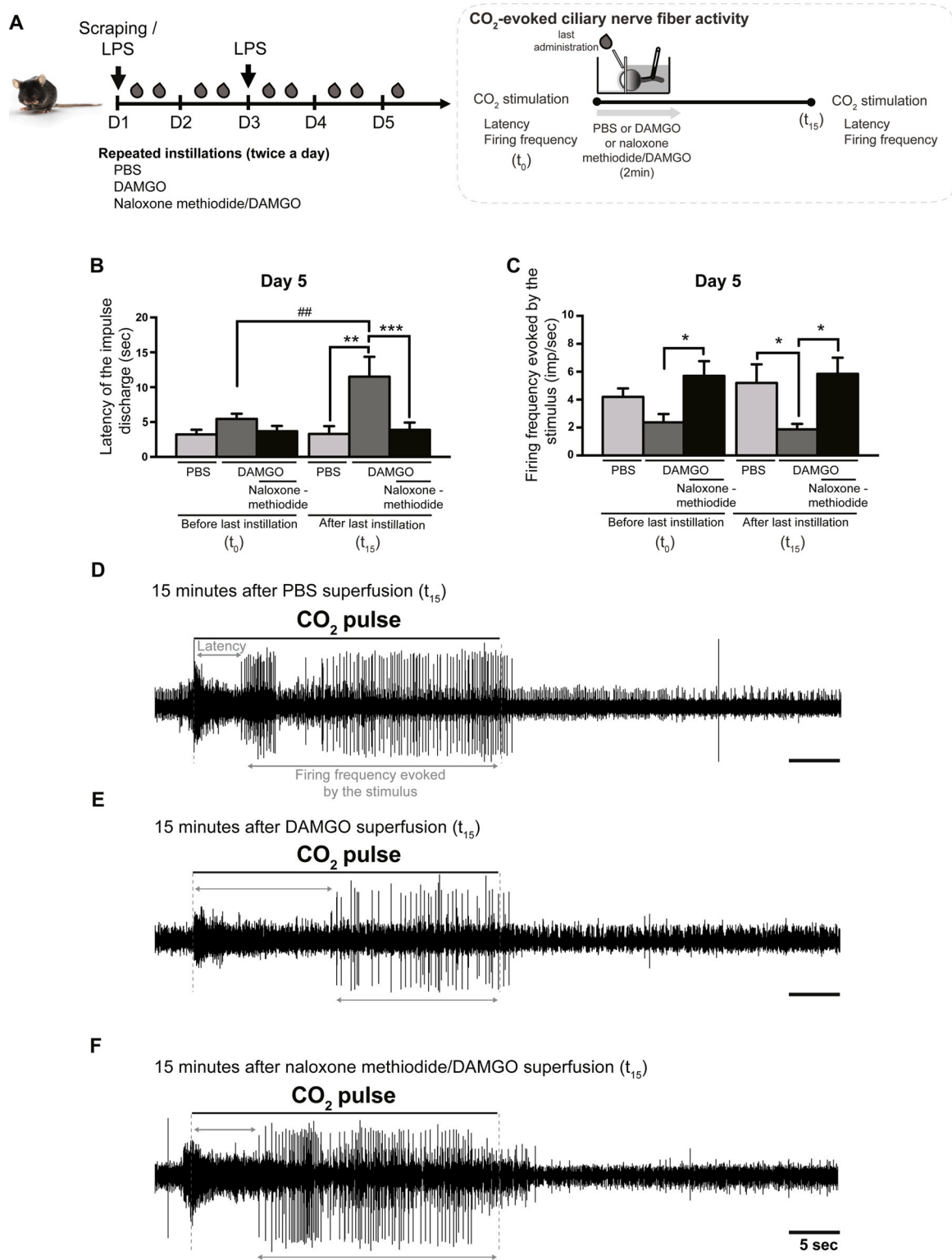


**Fig. 6.** Repeated instillations of DAMGO reduces the responsiveness of ciliary nerves to chemical stimulation in the inflammatory corneal pain model. (A) Schematic diagram of the experiments performed 5 days after scraping/LPS treatment. Time 0 ( $t_0$ ) and  $t_{15}$  values correspond to the latency of the impulse discharge or the firing frequency evoked by the stimulus, measured before and 15 min after drug superfusion, respectively. (B–C) Histograms showing the latency of the impulse discharge (B) and the mean firing frequency evoked by the CO<sub>2</sub> pulse stimulus (C) on D5 at  $t_0$  and  $t_{15}$  after PBS (light grey bars), DAMGO alone (dark grey bars), or naloxone methiodide followed by DAMGO (black bars) administration (D–F) Traces illustrating the corneal responsiveness to chemical stimulation, with a 30-s CO<sub>2</sub> pulse, 15 min after the superfusion of PBS (D), DAMGO (E), or naloxone methiodide followed by DAMGO (F). The black line represents the duration of the CO<sub>2</sub> pulse. N = 5–10 mice per group. The differences between groups were analyzed by one-way ANOVA, Kruskal and Wallis tests, or two-way ANOVA, depending on which was appropriate. \* indicates a significant difference between the DAMGO and PBS alone or naloxone methiodide followed by DAMGO. # indicates a significant difference between  $t_0$  and  $t_{15}$  after DAMGO instillation. \* $p < 0.05$ , \*\* $p < 0.01$ , \*\*\* $p < 0.001$ , # $p < 0.01$ .

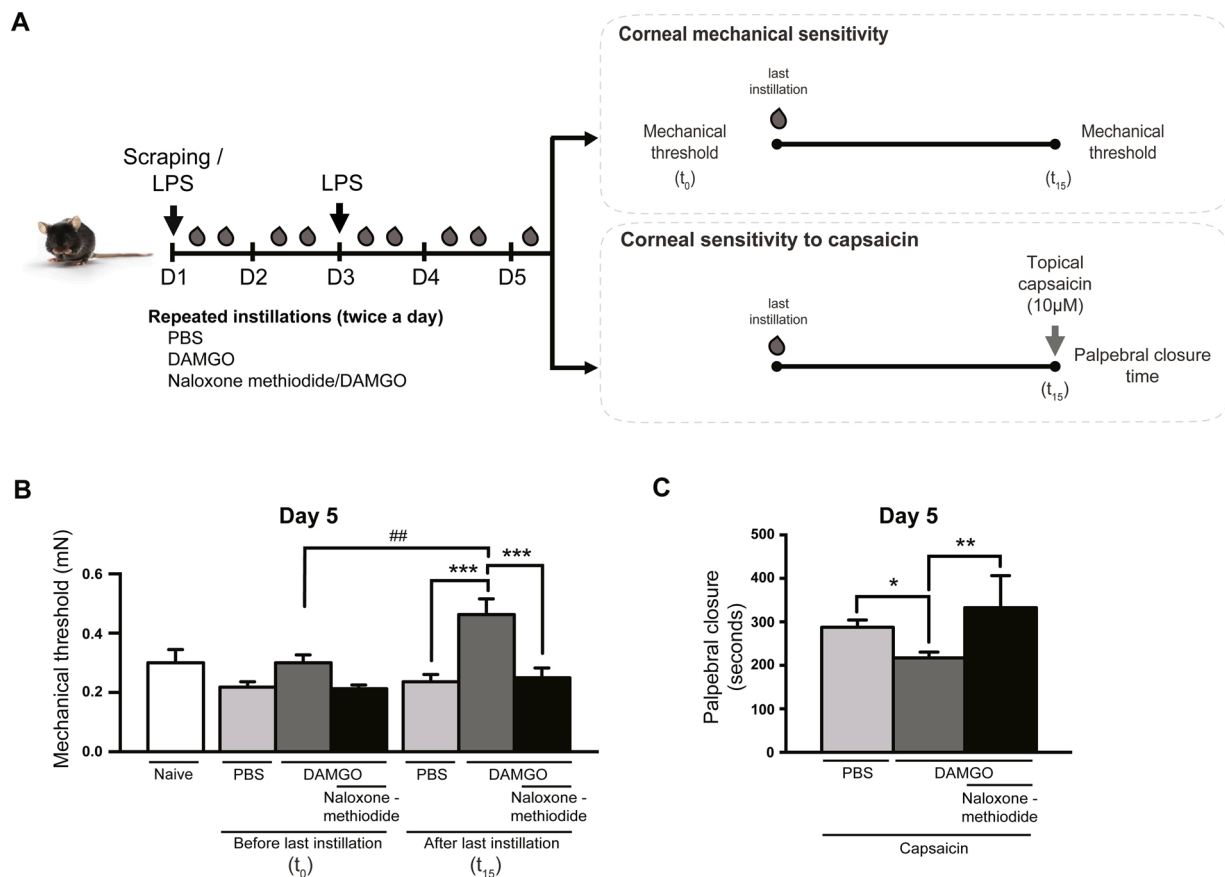


**Fig. 7.** Repeated topical instillations of DAMGO induces analgesic effects by decreasing the mechanical allodynia and pain induced by topical capsaicin. (A) Schematic diagram of the experiments. (B) Mechanical corneal sensitivity in naive mice (white bar) and on D5 after corneal scraping/LPS, before ( $t_0$ ) and 15 min ( $t_{15}$ ) after the last instillation of PBS (light gray bars), DAMGO alone (dark gray bars), or naloxone methiodide followed by DAMGO (black bars). (C) The palpebral closure time after deposition of a drop of capsaicin onto the cornea on D5, at  $t_{15}$  after the last instillation of PBS (light gray bar), DAMGO alone (dark gray bar), or naloxone methiodide followed by DAMGO (black bar).  $N = 8-11$  mice per group for mechanical corneal sensitivity 5–6 per group for the capsaicin test. The differences between groups were analyzed by one-way or two-way ANOVA, depending on which was appropriate. \* indicates a significant difference between the PBS, DAMGO, and naloxone methiodide/DAMGO groups. # indicates a significant difference between  $t_0$  (before) and  $t_{15}$  after DAMGO instillation. \* $p < 0.05$ , \*\* $p < 0.01$ , \*\*\* $p < 0.001$ , ## $p < 0.01$ .

pain, and (4) topical instillation of DAMGO prevents the increase of the spontaneous activity of ciliary nerve fibers associated with corneal inflammatory pain.

The management of ocular pain is still a therapeutic challenge and no specific pharmacological approaches to treat corneal pain are yet available. In the clinic, topical anesthetics are used to reduce acute pain, but their long-term use is not recommended due to their shortcomings (e.g., corneal ulceration) [37,38]. We recently demonstrated that repeated ocular administration of PL265, a dual inhibitor of the enkephalin-degrading enzymes, neutral endopeptidase and aminopeptidase N, exerts anti-nociceptive effects in several models of corneal pain [21]. This study revealed that targeting opioid receptors could be an effective approach to reduce corneal pain. However, it did not assess the contribution of the MOR, the potential changes of MOR expression in the cornea and TG neurons, or the beneficial effects of ocular administration of MOR agonists on corneal nerve-fiber activity and pain-like behavior.

Our anatomical data demonstrate, for the first time, that the MOR can be detected in the corneal nerves of mice. This observation is consistent with the study of Zollner, who reported MOR immunoreactivity of corneal nerves in the human cornea [39]. Moreover, clear staining was found in the small- and medium-sized neurons located in the ophthalmic branch of the TG. This is consistent with a previous finding of Ichikama, in which MOR immunoreactivity was also not found in small or medium-sized trigeminal neurons [40].

Several studies have reported that the expression of opioid receptors

increases under pathological conditions, such as injury and inflammation, leading to improved agonist efficacy of peripheral nerve terminals [36,41]. We observed a quantitative increase in MOR expression in the cornea and ophthalmic branch of TG under conditions of pain. These changes in MOR expression provide novel clues about the involvement and activation of the endogenous opioid system during inflammatory corneal pain.

Corneal sensory information is relayed by myelinated A-delta and unmyelinated C-fibers [33,42,43], which have a small diameter and respond to chemical, mechanical, and thermal noxious stimulation of the cornea. The presence of MORs, both in corneal nerves and the small afferent neurons of TG, provides an anatomical basis to support the possible modulation of MOR activity by MOR agonists. Although a large number of studies have proven that MOR agonists, such as DAMGO, reduce pain in various peripheral pain models [44,45], the topical analgesic effects of DAMGO in a corneal pain model are still unknown. Here, we provide evidence for the antinociceptive effects of DAMGO by showing reduced mechanical corneal allodynia and capsaicin-induced thermal hyperalgesia in mice. This last result is consistent with those of the study of Wenk [22], who reported that topical application of morphine attenuated capsaicin-induced blinking in acute chemical injury in rats.

Previous *in vivo* and whole-cell patch-clamp studies on dorsal root neurons have demonstrated that MOR activation decreases pain responses and capsaicin-induced TRPV1 currents in a naloxone-sensitive

manner [46]. Currently, it is difficult to determine whether MOR activation modifies TRPV1 currents in corneal nerve terminals, as previously reported in the primary sensory neuron in dorsal root ganglia. Further studies are necessary to test this hypothesis. Moreover, complete reversion of the antinociceptive effects of DAMGO by naloxone methiodide (a non-selective antagonist of opioid receptors that does not cross the blood-brain barrier [47]) confirms that the DAMGO-induced analgesic effects are mediated by peripheral MOR activation. The marked antinociceptive effect of DAMGO instillation, together with the increased expression of MOR in TG neurons, reinforces the hypothesis that the MORs within these structures are involved in the peripheral modulation of inflammatory pain noxious inputs.

*Ex vivo* and *in vivo* behavior (pain-like behavioral tests) demonstrated that mice treated with repeated topical ocular DAMGO do not develop exacerbated excitability of corneal afferents or mechanical hypersensitivity. This is in contrast to studies that observed increased sensitivity to pain after peripheral MOR activation and that repeated injection of DAMGO at the site of mechanical nociception testing (hind paw) produced changes in nociceptor function [48–50]. The differences between the aforementioned study and ours could be explained by the nature of the tissue (skin *versus* cornea) and the nociceptive pathways involved (dorsal root ganglion *vs* trigeminal ganglion).

A link between corneal nerve damage, inflammation, and the ongoing activity of corneal nerve fibers has been previously reported in various mouse models of corneal injury [10,30,51]. Here, we used a preclinical model of corneal inflammatory pain consisting of the combination of corneal scraping (corneal nerve damage) and LPS administration [21,51]. The two instillations of LPS at D1 and D3 were used to maintain the release of inflammatory mediators that activate and sensitize the nociceptive system. Both factors (inflammation and corneal nerve damage) are important for studies on the pathophysiological mechanisms of ocular inflammatory pain. In addition, this model is characterized by infiltration of the inflammatory monocyte/macrophage population (CD11b<sup>+</sup> cells) in the cornea [21], as confirmed by *in vivo* confocal microscopy. These recruited inflammatory cells ultimately release a number of proinflammatory cytokines, *i.e.*, IL-1, IL-6, and TNF- $\alpha$  [28,52], in the proximity of the corneal fibers. These local inflammatory responses could explain the increase of the nociceptive mechanical and chemical (capsaicin) sensitivity found in our scraping/LPS model. The infiltration of inflammatory cells is known to affect the activity of corneal nerve terminals, contributing to the sensitization of nociceptors and reducing the responsiveness of cold thermoreceptors [28,52]. Peripheral sensitization is characterized by a specific change in the excitability of these nerve fibers by an increase in their ongoing and stimulus-evoked nerve activity [2,53]. Thus, the increased ongoing firing activity of the ciliary nerve, observed in the scraping/LPS corneas on D5, may have largely resulted from changes in the excitability of the cold-sensitive nerve fibers induced by corneal injury. This is a condition that triggers TRPM8 channel expression and thus increases ongoing firing activity [2,51,54].

Another important finding from our experiments is that repeated topical instillation of DAMGO modulates the electrophysiological properties and activity of corneal neurons. Previous studies have reported that exogenous and endogenous opioids are able to attenuate the excitability or propagation of the action potentials of peripheral nociceptors [55,56]. Injection of DAMGO into the brainstem (Vc/C1 region) was shown to reduce the response of second-order corneal neurons to CO<sub>2</sub> stimulation of the cornea in rats [4]. Here, we demonstrate, for the first time, that repeated administration of DAMGO diminishes the increased spontaneous ciliary nerve activity associated with corneal pain, as well as the corneal polymodal response to CO<sub>2</sub> stimulation. The functional changes of the corneal polymodal nociceptors and cold thermoreceptors induced by DAMGO were entirely blunted by naloxone methiodide, demonstrating that the effects of DAMGO are directly mediated by MORs expressed by the corneal nerves. Importantly, these electrophysiological changes corroborate the analgesic effects

(decreased mechanical allodynia and topical capsaicin-induced pain) that we report here.

#### 4. Conclusions

We demonstrate that MOR expression increases in corneal nerve fibers and trigeminal neurons under conditions of corneal pain, as well as the beneficial effects of repeated ocular administration of DAMGO on corneal nerve hyperactivity and corneal allodynia. Our findings contribute to a literature suggesting that topical opioid agonists could be repurposed for the treatment of ocular pain. Thus, pharmacological activation of corneal MORs may be a potential therapeutic target for the treatment of inflammatory ocular pain.

#### Author contributions

F. Joubert designed and performed the experiments, analyzed and interpreted the data, generated the figures, discussed the results and their significance, and wrote the manuscript. A. Guerrero-Moreno performed the immunohistochemistry experiments and analyzed the *in situ* experiments. D. Fakhri performed the RNAscope experiments. E. Reboussin performed the confocal image acquisition. C. Gaveriaux-Ruff provided scientific input and commented on the manuscript. MC. Acosta and J. Gallar helped in the acquisition and analysis of the electrophysiological recordings and commented on the manuscript. JA. Sahel provided scientific input. L. Bodineau helped in the electrophysiological experiments and commented on the manuscript. C. Baudouin discussed the results and their significance and commented on the manuscript. W. Rostène discussed the results and their significance and commented on the manuscript. S. Melik-Parsadaniantz interpreted the data, discussed the results and their significance, and commented on the manuscript. A. Réaux-Le Goazigo designed and supervised all experiments, obtained the funding, interpreted the data, discussed the results and their significance, and wrote the manuscript. All authors approved the final version of the article.

#### Declaration of Competing Interest

The authors report no declarations of interest.

#### Acknowledgements

We thank Stéphane Fouquet (imagery platform) and the staff of the animal house facilities at the Institut de la Vision and Institut du Cerveau et de la Moelle for their help. We also thank Yanis Merabet for technical assistance with the UMB3 staining in the cornea and Katia Marazova for fruitful discussions. This work was supported by the Sorbonne Université and the Institut National de la Santé et de la Recherche Médicale, the ANR, LabEx LIFESENSES (ANR-10-LABX-65), and IHU FOrE-SIGHT (ANR-18-IAHU-01). Fanny Joubert was supported by a Fondation de France post-doc fellowship grant. Adrian Guerrero Moreno was funded by a H2020-MSCA-ETN program (IT-DED<sup>3</sup>) (Grant Agreement 765608). The text has been edited for English by Alex Edelman & Associate.

#### Appendix A. Supplementary data

Supplementary material related to this article can be found, in the online version, at doi:<https://doi.org/10.1016/j.biopha.2020.110794>.

#### References

- [1] F. Stapleton, M. Alves, V.Y. Bunya, I. Jalbert, K. Lekhanont, F. Malet, K.S. Na, D. Schaumberg, M. Uchino, J. Vehof, et al., TFOS DEWS II epidemiology report, *Ocul. Surf.* 15 (2017) 334–365.
- [2] A.E. Levitt, A. Galor, A.R. Chowdhury, E.R. Felix, C.D. Sarantopoulos, G.Y. Zhuang, D. Patin, W. Maixner, S.B. Smith, E.R. Martin, R.C. Levitt, Evidence that dry eye

- represents a chronic overlapping pain condition, *Mol. Pain* 13 (2017), 1744806917729306.
- [3] A. Galor, H.R. Moein, C. Lee, A. Rodriguez, E.R. Felix, K.D. Sarantopoulos, R. C. Levitt, Neuropathic pain and dry eye, *Ocul. Surf.* 16 (2018) 31–44.
- [4] H. Hirata, S. Takeshita, J.W. Hu, D.A. Bereiter, Cornea-responsive medullary dorsal horn neurons: modulation by local opioids and projections to thalamus and brain stem, *J. Neurophysiol.* 84 (2000) 1050–1061.
- [5] A.J. Rozsa, R.W. Beuerman, Density and organization of free nerve endings in the corneal epithelium of the rabbit, *Pain* 14 (1982) 105–120.
- [6] C.F. Marfurt, R.E. Kingsley, S.E. Echtenkamp, Sensory and sympathetic innervation of the mammalian cornea. A retrograde tracing study, *Invest. Ophthalmol. Vis. Sci.* 30 (1989) 461–472.
- [7] J.J. Ivanusic, R.J. Wood, J.A. Brock, Sensory and sympathetic innervation of the mouse and guinea pig corneal epithelium, *J. Comp. Neurol.* 521 (2013) 877–893.
- [8] C.F. Marfurt, D.R. Del Toro, Corneal sensory pathway in the rat: a horseradish peroxidase tracing study, *J. Comp. Neurol.* 261 (1987) 450–459.
- [9] P.S. Launay, D. Godefroy, H. Khabou, W. Rostene, J.A. Sahel, C. Baudouin, S. Melik-Parsadaniantz, Reaux-Le Goazigo A: combined 3DISCO clearing method, retrograde tracer and ultramicroscopy to map corneal neurons in a whole adult mouse trigeminal ganglion, *Exp. Eye Res.* (2015).
- [10] F. Joubert, M.D.C. Acosta, J. Gallar, D. Fakh, J.A. Sahel, C. Baudouin, L. Bodineau, S. Melik Parsadaniantz, Reaux-Le Goazigo A: effects of corneal injury on ciliary nerve fibre activity and corneal nociception in mice: a behavioural and electrophysiological study, *Eur. J. Pain* 23 (2019) 589–602.
- [11] M.C. Acosta, C. Luna, S. Quirce, C. Belmonte, J. Gallar, Corneal sensory nerve activity in an experimental model of UV keratitis, *Invest. Ophthalmol. Vis. Sci.* 55 (2014) 3403–3412.
- [12] S. Gonzalez-Rodriguez, M.A. Quadir, S. Gupta, K.A. Walker, X. Zhang, V. Spahn, D. Labuz, A. Rodriguez-Gaztelumendi, M. Schmelz, J. Joseph, et al., Polyglycerol-opioid conjugate produces analgesia devoid of side effects, *Elife* (2017) 6.
- [13] C. Stein, M. Schafer, A.H. Hassan, Peripheral opioid receptors, *Ann. Med.* 27 (1995) 219–221.
- [14] E. Erbs, L. Faget, G. Scherrer, A. Matifas, D. Filliol, J.L. Vonesch, M. Koch, P. Kessler, D. Hentsch, M.C. Birling, et al., A mu-delta opioid receptor brain atlas reveals neuronal co-occurrence in subcortical networks, *Brain Struct. Funct.* 220 (2015) 677–702.
- [15] D. Wang, V.L. Tawfik, G. Corder, S.A. Low, A. Francois, A.I. Basbaum, G. Scherrer, Functional divergence of Delta and mu opioid receptor organization in CNS pain circuits, *Neuron* 98 (2018) 90–108, e105.
- [16] C. Gaveriaux-Ruff, Opiate-induced analgesia: contributions from mu, delta and kappa opioid receptors mouse mutants, *Curr. Pharm. Des.* 19 (2013) 7373–7381.
- [17] P. Richebe, A. Cahana, C. Rivat, Tolerance and opioid-induced hyperalgesia. Is a divorce imminent? *Pain* 153 (2012) 1547–1548.
- [18] V.B.P. Pereira, R. Garcia, A.A.M. Torricelli, A. Mukai, S.J. Bechara, Codeine plus acetaminophen for pain after photorefractive keratectomy: a randomized, double-blind, placebo-controlled add-on trial, *Cornea* 36 (2017) 1206–1212.
- [19] G. Dieckmann, S. Goyal, P. Hamrah, Neuropathic corneal pain: approaches for management, *Ophthalmology* 124 (2017) S34–S47.
- [20] A.N. Siedlecki, S.D. Smith, A.R. Siedlecki, S.M. Hayek, R.R. Sayegh, Ocular pain response to treatment in dry eye patients, *Ocul. Surf.* 18 (2020) 305–311.
- [21] A. Reaux-Le Goazigo, H. Poras, C. Ben-Dhaou, T. Ouimet, C. Baudouin, M. Wurm, Melik Parsadaniantz S: dual enkephalinase inhibitor PL265: a novel topical treatment to alleviate corneal pain and inflammation, *Pain* 160 (2019) 307–321.
- [22] H.N. Wenk, M.N. Nanneng, C.N. Honda, Effect of morphine sulphate eye drops on hyperalgesia in the rat cornea, *Pain* 105 (2003) 455–465.
- [23] S.M. Thomson, J.A. Oliver, D.J. Gould, M. Mendl, E.A. Leece, Preliminary investigations into the analgesic effects of topical ocular 1% morphine solution in dogs and cats, *Vet. Anaesth. Analg.* 40 (2013) 632–640.
- [24] J. Stiles, C.N. Honda, S.G. Krohne, E.A. Kazacos, Effect of topical administration of 1% morphine sulfate solution on signs of pain and corneal wound healing in dogs, *Am. J. Vet. Res.* 64 (2003) 813–818.
- [25] G.A. Peyman, M.H. Rahimy, M.L. Fernandes, Effects of morphine on corneal sensitivity and epithelial wound healing: implications for topical ophthalmic analgesia, *Br. J. Ophthalmol.* 78 (1994) 138–141.
- [26] E.G. Faktorovich, A.I. Basbaum, Effect of topical 0.5% morphine on postoperative pain after photorefractive keratectomy, *J. Refract. Surg.* 26 (2010) 934–941.
- [27] R. Moshourab, C. Stein, Fentanyl decreases discharges of C and A nociceptors to suprathreshold mechanical stimulation in chronic inflammation, *J. Neurophysiol.* 108 (2012) 2827–2836.
- [28] P.S. Launay, E. Reboussin, H. Liang, K. Kessal, D. Godefroy, W. Rostene, J.A. Sahel, C. Baudouin, S. Melik Parsadaniantz, A. Reaux Le Goazigo, Ocular inflammation induces trigeminal pain, peripheral and central neuroinflammatory mechanisms, *Neurobiol. Dis.* 88 (2016) 16–28.
- [29] M.C. Acosta, C. Luna, S. Quirce, C. Belmonte, J. Gallar, Changes in sensory activity of ocular surface sensory nerves during allergic keratoconjunctivitis, *Pain* 154 (2013) 2353–2362.
- [30] D. Fakh, Z. Zhao, P. Nicole, E. Reboussin, F. Joubert, J. Luzu, A. Labbe, W. Rostene, C. Baudouin, S. Melik Parsadaniantz, A. Reaux-Le Goazigo, Chronic dry eye induced corneal hypersensitivity, neuroinflammatory responses, and synaptic plasticity in the mouse trigeminal brainstem, *J. Neuroinflammation* 16 (2019) 268.
- [31] F. Bech, O. Gonzalez-Gonzalez, E. Artime, J. Serrano, I. Alcalde, J. Gallar, J. Merayo-Llives, C. Belmonte, Functional and morphologic alterations in mechanical, polymodal, and cold sensory nerve fibers of the Cornea Following Photorefractive Keratectomy, *Invest. Ophthalmol. Vis. Sci.* 59 (2018) 2281–2292.
- [32] J. He, T.L. Pham, A.H. Kakazu, H.E.P. Bazan, Remodeling of substance P sensory nerves and transient receptor potential melastatin 8 (TRPM8) cold receptors after corneal experimental surgery, *Invest. Ophthalmol. Vis. Sci.* 60 (2019) 2449–2460.
- [33] A. Alamri, R. Bron, J.A. Brock, J.J. Ivanusic, Transient receptor potential cation channel subfamily V member 1 expressing corneal sensory neurons can be subdivided into at least three subpopulations, *Front. Neuroanat.* 9 (2015) 71.
- [34] A. Lupp, N. Richter, C. Doll, F. Nagel, S. Schulz, UMB-3, a novel rabbit monoclonal antibody, for assessing mu-opioid receptor expression in mouse, rat and human formalin-fixed and paraffin-embedded tissues, *Regul. Pept.* 167 (2011) 9–13.
- [35] Y. Cui, S.B. Ostlund, A.S. James, C.S. Park, W. Ge, K.W. Roberts, N. Mittal, N. P. Murphy, C. Cepeda, B.L. Kieffer, et al., Targeted expression of mu-opioid receptors in a subset of striatal direct-pathway neurons restores opiate reward, *Nat. Neurosci.* 17 (2014) 254–261.
- [36] C. Stein, S. Kuchler, Targeting inflammation and wound healing by opioids, *Trends Pharmacol. Sci.* 34 (2013) 303–312.
- [37] J.P. Harnisch, F. Hoffmann, L. Dumitrescu, Side-effects of local anesthetics on the corneal epithelium of the rabbit eye, *Albrecht Von Graefes Arch. Klin. Exp. Ophthalmol.* 197 (1975) 71–81.
- [38] G. Rocha, I. Brunette, M. Le Francois, Severe toxic keratopathy secondary to topical anesthetic abuse, *Can. J. Ophthalmol.* 30 (1995) 198–202.
- [39] C. Zollner, S. Mousa, A. Klinger, M. Forster, M. Schafer, Topical fentanyl in a randomized, double-blind study in patients with corneal damage, *Clin. J. Pain* 24 (2008) 690–696.
- [40] H. Ichikawa, S. Schulz, V. Holt, Z. Mo, M. Xiang, T. Sugimoto, Effect of Brn-3a deficiency on primary nociceptors in the trigeminal ganglion, *Neurosci. Res.* 51 (2005) 445–451.
- [41] R. Weibel, D. Reiss, L. Karchewski, O. Gardon, A. Matifas, D. Filliol, J.A. Becker, J. N. Wood, B.L. Kieffer, C. Gaveriaux-Ruff, Mu opioid receptors on primary afferent nav1.8 neurons contribute to opiate-induced analgesia: insight from conditional knockout mice, *PLoS One* (2013) 8, e74706.
- [42] A. Nakamura, T. Hayakawa, S. Kuwahara, S. Maeda, K. Tanaka, M. Seki, O. Mimura, Morphological and immunohistochemical characterization of the trigeminal ganglion neurons innervating the cornea and upper eyelid of the rat, *J. Chem. Neuroanat.* 34 (2007) 95–101.
- [43] C. Belmonte, J.J. Nichols, S.M. Cox, J.A. Brock, C.G. Begley, D.A. Bereiter, D. A. Dartt, A. Galor, P. Hamrah, J.J. Ivanusic, et al., TFOS DEWS II pain and sensation report, *Ocul. Surf.* 15 (2017) 404–437.
- [44] P. Armenian, K.T. Vo, J. Barr-Walker, K.L. Lynch, Fentanyl, fentanyl analogs and novel synthetic opioids: a comprehensive review, *Neuropharmacology* 134 (2018) 121–132.
- [45] H. Beaudry, D. Dubois, L. Gendron, Activation of spinal mu- and delta-opioid receptors potentially inhibits substance P release induced by peripheral noxious stimuli, *J. Neurosci.* 31 (2011) 13068–13077.
- [46] J. Endres-Becker, P.A. Heppenstall, A.A. Mousa, D. Labuz, A. Oksche, M. Schafer, C. Stein, C. Zollner, Mu-opioid receptor activation modulates transient receptor potential vanilloid 1 (TRPV1) currents in sensory neurons in a model of inflammatory pain, *Mol. Pharmacol.* 71 (2007) 12–18.
- [47] S. Van Dorpe, A. Adriaens, I. Polis, K. Peremans, J. Van Bocxlaer, B. De Spiegeleer, Analytical characterization and comparison of the blood-brain barrier permeability of eight opioid peptides, *Peptides* 31 (2010) 1390–1399.
- [48] D. Araldi, L.F. Ferrari, J.D. Levine, Hyperalgesic priming (type II) induced by repeated opioid exposure: maintenance mechanisms, *Pain* 158 (2017) 1204–1216.
- [49] D. Araldi, L.F. Ferrari, J.D. Levine, Repeated mu-opioid exposure induces a novel form of the hyperalgesic priming model for transition to chronic pain, *J. Neurosci.* 35 (2015) 12502–12517.
- [50] G. Corder, D.C. Castro, M.R. Bruchas, G. Scherrer, Endogenous and exogenous opioids in pain, *Annu. Rev. Neurosci.* 41 (2018) 453–473.
- [51] R. Pina, G. Ugarte, M. Campos, A. Inigo-Portugues, E. Olivares, P. Orio, C. Belmonte, J. Bacigalupo, R. Madrid, Role of TRPM8 channels in altered cold sensitivity of corneal primary sensory neurons induced by axonal damage, *J. Neurosci.* 39 (2019) 8177–8192.
- [52] H. Liang, F. Brignole-Baudouin, A. Labbe, A. Pauly, J.M. Warnet, C. Baudouin, LPS-stimulated inflammation and apoptosis in corneal injury models, *Mol. Vis.* 13 (2007) 1169–1180.
- [53] M. Costigan, A. Moss, A. Latremoliere, C. Johnston, M. Verma-Gandhu, T. A. Herbert, L. Barrett, G.J. Brenner, D. Vardeh, C.J. Woolf, M. Fitzgerald, T-cell infiltration and signaling in the adult dorsal spinal cord is a major contributor to neuropathic pain-like hypersensitivity, *J. Neurosci.* 29 (2009) 14415–14422.
- [54] I. Kovacs, C. Luna, S. Quirce, K. Mizerska, G. Callejo, A. Riestra, L. Fernandez-Sanchez, V.M. Meseguer, N. Cuenca, J. Merayo-Llives, et al., Abnormal activity of corneal cold thermoreceptors underlies the unpleasant sensations in dry eye disease, *Pain* 157 (2016) 399–417.
- [55] Q. Cai, C.Y. Qiu, F. Qiu, T.T. Liu, Z.W. Qu, Y.M. Liu, W.P. Hu, Morphine inhibits acid-sensing ion channel currents in rat dorsal root ganglion neurons, *Brain Res.* 1554 (2014) 12–20.
- [56] B. Oehler, M. Mohammadi, C. Perpina Viciano, D. Hackel, C. Hoffmann, A. Brack, H.L. Rittner, Peripheral interaction of resolvin D1 and E1 with opioid receptor antagonists for antinociception in inflammatory pain in rats, *Front. Mol. Neurosci.* 10 (2017) 242.